RESEARCH ARTICLE

Ligand uptake in *Mycobacterium tuberculosis* truncated hemoglobins is controlled by both internal tunnels and active site water molecules [v1; ref status: approved 1, http://f1000r.es/4vq]

Ignacio Boron[1*], Juan Pablo Bustamante[2*], Kelly S Davidge[3], Sandip Singh[4], Lesley AH Bowman[5], Mariana Tinajero-Trejo[6], Sebastián Carballal[7], Rafael Radi[7], Robert K Poole[6], Kanak Dikshit[4], Dario A Estrin[2], Marcelo A Marti[1], Leonardo Boechi[8]

[1]Departamento de Química Biológica, Facultad de Ciencias Exactas y Naturales, Universidad de Buenos Aires, Buenos Aires, C1428EGA, Argentina
[2]Departamento de Química Inorgánica, Analítica y Química Física, INQUIMAE-CONICET, Facultad de Ciencias Exactas y Naturales, Universidad de Buenos Aires, Buenos Aires, C1428EGA, Argentina
[3]Centre for Biomolecular Sciences, The University of Nottingham, Nottingham, NG7 2RD, UK
[4]Institute of Microbial Technology, CSIR, Chandigarh, 160036, India
[5]Sir William Dunn School of Pathology, University of Oxford, Oxford, OX1 3RE, UK
[6]Molecular Biology and Biotechnology, The University of Sheffield, Sheffield, S10 2TN, UK
[7]Departamento de Bioquímica and Center for Free Radical and Biomedical Research, Facultad de Medicina, Universidad de la República, Montevideo, 11100, Uruguay
[8]Instituto de Cálculo, Facultad de Ciencias Exactas y Naturales, Universidad de Buenos Aires, Buenos Aires, C1428EGA, Argentina

[*] Equal contributors

v1 **First published:** 23 Jan 2015, **4**:22 (doi: 10.12688/f1000research.5921.1)
Latest published: 23 Jan 2015, **4**:22 (doi: 10.12688/f1000research.5921.1)

Abstract

Mycobacterium tuberculosis, the causative agent of human tuberculosis, has two proteins belonging to the truncated hemoglobin (trHb) family. Mt-trHbN presents well-defined internal hydrophobic tunnels that allow O_2 and •NO to migrate easily from the solvent to the active site, whereas Mt-trHbO possesses tunnels that are partially blocked by a few bulky residues, particularly a tryptophan at position G8. Differential ligand migration rates allow Mt-trHbN to detoxify •NO, a crucial step for pathogen survival once under attack by the immune system, much more efficiently than Mt-trHbO. In order to investigate the differences between these proteins, we performed experimental kinetic measurements, •NO decomposition, as well as molecular dynamics simulations of the wild type *Mt-trHbN* and two mutants, VG8F and VG8W. These mutations introduce modifications in both tunnel topologies and affect the incoming ligand capacity to displace retained water molecules at the active site. We found that a single mutation allows Mt-trHbN to acquire ligand migration rates comparable to those observed for Mt-trHbO, confirming that ligand migration is regulated by the internal tunnel architecture as well as by water molecules stabilized in the active site.

Open Peer Review

Referee Status: ✓

	Invited Referees 1
version 1 published 23 Jan 2015	✓ report

1 **Marco Nardini**, University of Milan Italy

Discuss this article

Comments (0)

Corresponding author: Leonardo Boechi (lboechi@ic.fcen.uba.ar)

How to cite this article: Boron I, Bustamante JP, Davidge KS *et al.* **Ligand uptake in *Mycobacterium tuberculosis* truncated hemoglobins is controlled by both internal tunnels and active site water molecules [v1; ref status: approved 1, http://f1000r.es/4vq]** *F1000Research* 2015, **4**:22 (doi: 10.12688/f1000research.5921.1)

Grant information: This work was supported by Framework program 7 NOstress Grant, CONICET, University of Buenos Aires, and Agencia Nacional de Promoción Científica y Tecnológica, National Institutes of Health Grant R01AI095173 and Universidad de la República (CSIC, Uruguay) to R. R. Additional funding to SC and RR was provided by PEDECIBA (Progama de Desarrollo de Ciencias Básicas, Uruguay) and CeBEM (Centro de Biología Estructural del Mercosur). IB and JPB hold CONICET PhD fellowships. LB is a Pew Latin American Fellow. LB, DAE and MAM are members of CONICET.
The funders had no role in study design, data collection and analysis, decision to publish, or preparation of the manuscript.

Competing interests: No competing interests were disclosed.

First published: 23 Jan 2015, **4**:22 (doi: 10.12688/f1000research.5921.1)

Introduction

Mycobacterium tuberculosis, the causative agent of human tuberculosis, affects approximately two billion people world-wide, causing over three millions deaths each year[1]. The genome of this pathogenic organism includes two genes, *glbN* and *glbO*, which encode for two proteins, termed here truncated hemoglobin N (Mt-trHbN) and truncated hemoglobin O (Mt-trHbO), belonging to the truncated hemoglobin (trHb) family of heme proteins, widely distributed in eubacteria, cyanobacteria, microbial eukaryotes and plants[2,3].

The truncated hemoglobin family exhibits a three-dimensional structure similar to the common globin fold of myoglobin, but significantly smaller. The secondary structure of trHbs consists of four α-helices arranged in a two-over-two antiparallel sandwich instead of the common three-over-three helix globin fold. Phylogenetic analysis has distinguished three different groups of truncated hemoglobins, classified as groups I, II and III, also called N, O and P, respectively.

It has been shown that group I Mt-trHbN catalyzes the detoxification of •NO in the presence of O_2[4,5]. The first step of this mechanism involves O_2 migration and binding. Subsequently, •NO migrates to the active site and reacts with the heme-bound O_2 to yield an unstable peroxynitrite adduct, which isomerizes to generate the relatively innocuous nitrate anion.

Several studies have examined the role of internal tunnels in ligand migration in trHbs[2,5–8]. Three internal tunnels were found in the truncated hemoglobin family: a long tunnel (LT) topologically positioned between helices B and E, and two short tunnels, known as the E7 Gate (E7 gate) and the short tunnel G8 (STG8), which are roughly normal to the LT, as depicted in Figure 1. The E7 tunnel corresponds to the highly conserved E7 pathway widely studied in both myoglobin and hemoglobin[9–11]. The STG8 tunnel is analogous to that found in Mt-trHbN, next to the key residues VG8 and IH11.

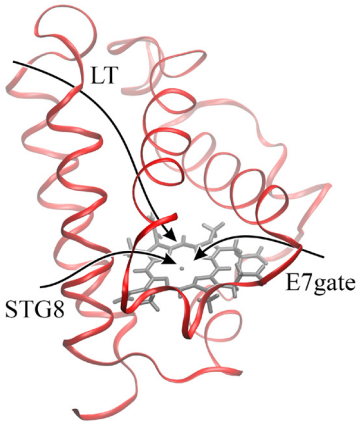

Figure 1. Schematic representation of the potential tunnels described in truncated hemoglobins. The three pathways, Long Tunnel (LT), E7 Gate (E7 gate) and Short Tunnel G8 (STG8) for ligand migration through the tertiary structure of a typical trHb are shown.

Previous results indicate that WG8, an absolutely conserved residue in groups II and III truncated hemoglobins, is involved in hindering ligand migration in Mt-trHbO by blocking both STG8 and LT (Figure 1)[12–14]. In addition, the presence of a smaller residue at the G8 position in the Mt-trHbO mutant (WG8F) was observed to increase the small ligand association constant, although the molecular details of this process were not investigated[12–14]. It has also been noted that internal water molecules can block the heme accessibility, thus delaying ligand binding[15–17].

By performing CO association kinetic constant measurements (k_{on} *CO*), •NO decomposition, and molecular dynamics (MD) simulations, we addressed molecular mechanisms that control ligand association in *M. tuberculosis* truncated hemoglobins.

Materials and methods

Site-directed mutant construction

The trHbN G8 mutants (VG8W and VG8F) were prepared using the Stratagene QuikChange mutagenesis kit. The following primers were designed using Primer3 http://biotools.umassmed.edu/bioapps/primer3_www.cgi[18] to generate single amino acid substitutions (underlined): i) WG8: forward primer 5'–CACTTCAGCCTGTGG GCCGGACACTTGG–3' and reverse primer 5'–CAAGTGTCC GGCCCACAGGCTGAAGTG–3'; ii) FG8: forward primer 5'–ACCACTTCAGCCTGTTCGCCGGACACTTG–3' and reverse primer 5'–CAAGTGTCCGGCGAACAGGCTGAAGTGGT–3'. Polymerase chain reaction (PCR) amplification of pET9b carrying the glbN gene with the aforementioned primers was conducted following manufacturer's instructions. The PCR mix consisted of 5 µl 10x reaction buffer, 5–50 ng double stranded DNA template, 125 ng oligonucleotide primer 1, 125 ng oligonucleotide primer 2, 1 µl dNTP mix, 1 µl *PfuUltra* HF DNA polymerase and double distilled H_2O to a final volume of 50 µl. The PCR reaction was 95°C for 30 s, followed by 16 cycles of: 95°C for 30 s, 55°C for 1 min and 68°C for 4 min. The reaction mix was then digested with DpnI to remove parental methylated DNA. Plasmid containing the mutated gene was then purified and used to transform *Escherichia coli* XL-1 Blue electrocompetent cells. Cells were provided by Invitrogen. Constructs were checked by sequencing.

Protein purification

All chemicals and reagents were obtained from Sigma Aldrich, unless indicated otherwise. The trHbN protein was purified using standard techniques reported for other bacterial globins[19]. Briefly, mutated constructs were used to transform *E. coli* BL21 DE3 pLysS. Starter cultures grown overnight in LB supplemented with kanamycin (50 µg ml^{-1}) and chloramphenicol (35 µg ml^{-1}) were used to inoculate 6 batches of 1 L LB medium at 1% (v/v), supplemented with kanamycin and 3 µM $FeCl_3$. Once cultures reached an OD_{600} of around 0.4, expression of trHbN was initiated by the addition of 1 mM IPTG and grown for a further 4 h. Cells were harvested by centrifugation at 5500 rpm for 20 min at 4°C and stored overnight at -20°C. After thawing, cells were resuspended in 40 ml buffer (10 mM TRIS-HCl (pH 7.0) with 1 mM EDTA, 10 mM DTT, 45 µg ml^{-1} phenylmethylsulphonyl fluoride, 500 µg ml^{-1} RNase and 50 µl DNase), homogenized using a Douce homogeniser and

ultracentrifuged at 44,000 rpm for 1 h at 4°C. The supernatant, red in color, was loaded onto a 30 ml DEAE Sepharose Fast Flow column (Pharmacia Biotech) equilibrated with 10 mM TRIS-HCl (pH 7.0), washed with the same buffer until the UV trace returned to baseline, and eluted via a gradient from 0 to 1 M NaCl in 10 mM TRIS-HCl using an Akta purifier (GE Healthcare Bio-Sciences, Amersham Biosciences, U.K. Ltd.). Fractions that were most red in color were concentrated using a Vivaspin 20 concentrator (Sartorius Stedim Biotech) to around 5 ml and loaded onto a gel filtration Superdex 75 column, equilibrated with 0.15 M NaCl in 10 mM TRIS-HCl (pH 7.5); again, fractions with the most color were collected, combined and stored at -80°C. Purity was checked using gel electrophoresis and analysis of the heme-to-protein ratio (410 nm and 280 nm in the UV-visible absorption spectrum).

Kinetic stopped flow measurements of CO binding

Rapid mixing experiments were conducted with a thermostated stopped flow apparatus (BioLogic SFM-300). Kinetics of carbon monoxide (CO) binding to determine the k_{on} *CO* were measured on the deoxy state of mutant and wild type globins at 20ºC. Solutions containing 5 µM protein in a 100 mM sodium phosphate at pH 7.0 were degassed in a nitrogen atmosphere and reduced with an equimolar concentration of sodium dithionite and mixed with increasing CO concentrations. The observed pseudo first-order rate constant (k_{obs}) was determined by fitting the absorbance decay resulting from association of the protein with CO, to a single exponential function. Kinetic rate constants (k_{on} *CO*) were obtained from the slope of the plots of k_{obs} as a function of CO concentration.

•NO decomposition

To determine rates of nitric oxide (•NO) decomposition by wild type and mutant Mt-trHbN proteins, •NO was added, as ProliNONOate, to a solution of 50 mM KPi buffer with 50 µM EDTA (pH 7.5), 100 µM NADPH and 100 nM *E. coli* ferredoxin reductase inside a thermoregulated, magnetically stirred reaction vessel. Mt-trHbN (2 µM) was added at the apex of the signal response to 2 µM ProliNONOate and •NO decay was followed until depleted using an •NO electrode (World Precision Instruments). Rates of •NO decay were calculated for each protein by determining the time taken for peak •NO concentrations to decay by 0.5 µM and were expressed per µM heme, determined spectrally by the peak in the Soret region at 410 nm.

Set up of the simulations

The starting structure corresponds to Mt-trHbN crystal structure (PDB entry 1IDR http://www.rcsb.org/pdb/explore/explore.do?structureId=1IDR), at 1.9 Å of resolution[20]. Amino acids protonation states were assumed based on environment of the residue in the crystal structure. All the solvent-exposed His were protonated at the N-δ delta atom, as well as HisF8, because of its coordination to the heme iron. An octahedral box of 10 Å of radius, which corresponds to 5234 explicit water molecules was added to the system. TIP3P water molecules were used by tLEaP module of the AMBER12 package[21]. The param99 Amber force field was used for all the aminoacid parameters[22] except heme parameters which were developed in our group[23] and strongly validated for being used in several studies of heme proteins[24–30]. Periodic boundary conditions were used for all the simulations performed with a 9 Å cutoff. Particle mesh Ewald (PME) summation method for treating the electrostatic interactions. The SHAKE algorithm was used to keep constant the non-polar hydrogen equilibrium distance. Temperature and pressure were kept constant with Langevin thermostat and barostat, respectively, as implemented in the AMBER12 program[21]. The equilibration simulation protocol was performed as follow: (i) slowly heating the system from 0 to 300K for 20 ps at constant volume, by using harmonic restraints of 80 kcal/mol A^2 for all C_α atoms and (ii) pressure equilibration of the whole system during 1 ns at 300K with restrained atoms in (i). (iii) Unconstrained 100 ns molecular dynamics simulation at constant temperature (300K) was performed.

In silico mutant proteins were built by using tLEaP module of AMBER12 package[21], and underwent the same protocol used for wild type protein. Root Mean Square Deviation (RMSD) was used as structure stability controls. All structures were observed to be stables during the time scale of the simulation (Figure S1).

Ligand migration free energy profiles

The free energy profile for the CO migration process inside the protein tunnel/cavity system was computed by the Implicit Ligand Sampling (ILS) approach that post-processes, using a probe molecule, an MD simulation performed in the absence of the ligand. This method was thoroughly tested for heme proteins[32]. ILS calculations were performed on a rectangular grid (0.5 Å resolution) that includes the whole simulation box (i.e. protein and the solvent) and the probe used was a CO molecule. Calculations were performed on 5000 frames taken from the last 90 ns of simulation time. The values for grid size, resolution and frame numbers were tested in a previous study[32]. Analysis of the ILS data was performed using an *ad-hoc* fortran-90 program available upon request[32]. Moreover, ILS has been shown to yield quantitative results for ligand migration processes when compared with more costly free energy methods that treat the ligand explicitly.

Results

CO association kinetic constant measurements

Although CO is not the natural ligand of the hemeproteins, it is widely used as a probe for ligand association studies due to its ease of use. In order to address the molecular determinants controlling ligand migration we performed CO ligand association constant measurements of wild type Mt-trHbN and two mutants: VG8F and VG8W. Kinetic traces for CO binding were measured through the absorption changes at the CO adduct peak position (λ=423 nm; Figure 2). Association of CO is well described by a single exponential decay, whose rate constant (k_{obs}) depends linearly on CO concentration and the slope can be interpreted as k_{on} *CO*. A significant k_{on} *CO* decrease for VG8F (715 ± 27 $mM^{-1}s^{-1}$), and an even larger decrease for VG8W (48 ± 1 $mM^{-1}s^{-1}$) was observed in relation to that observed for the wild type protein (4495 ± 357 $mM^{-1}s^{-1}$) (Figure 3). Table 1 summarizes the measured k_{on} *CO* values for wild type and mutant Mt-trHbs O and N, and is presented alongside literature data.

Molecular dynamics simulations

Small ligand association in the trHb family is presumably regulated by two main processes: i) ligand migration from solvent bulk to the

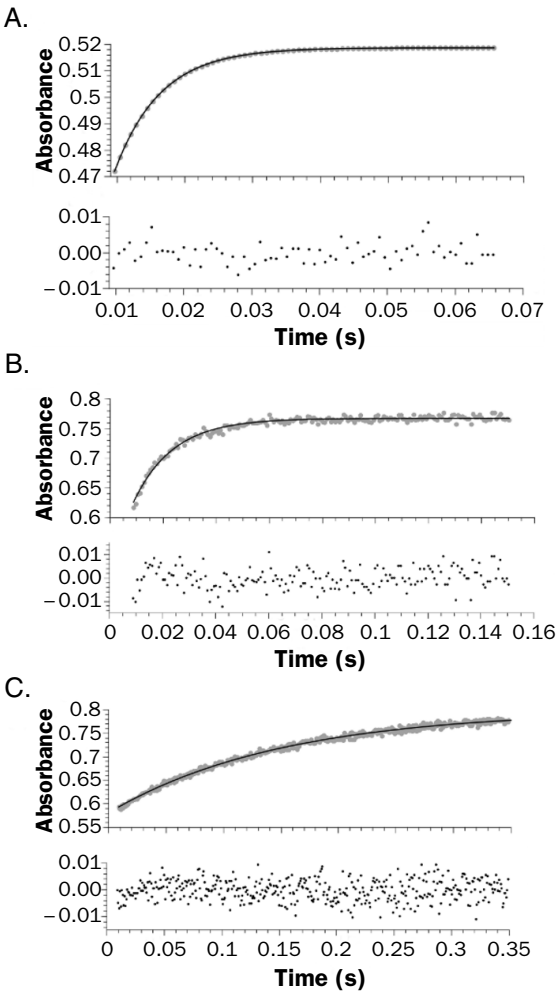

Figure 2. Stopped-flow time course for the reaction of reduced 5 μM wild type (**A**), VG8F (**B**), and VG8W (**C**) mutants in 100 mM phosphate buffer at pH 7. The reaction was monitored at 423 nm (grey dots) and the line shows the best first order fit.

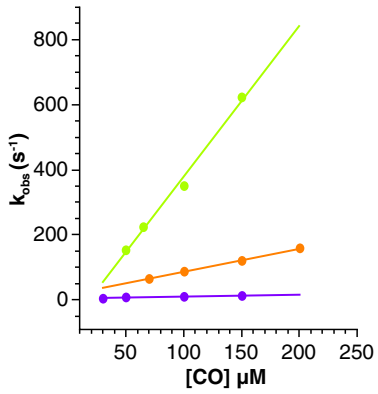

Figure 3. Apparent rates k_{obs} for CO binding to ferrous Mt-trHbN. Curves for wild type (green), VG8F (orange) and VG8W (violet) mutants as a function of CO concentration in stopped flow measurements are shown. The time courses are measured at different CO concentrations ranging from 10 to 200 μM (after mixing). Continuous line corresponds to linear fit of k_{obs} rates.

Table 1. Association kinetic constants for wild type and mutant Mt-trHbs O and N.

Protein	k_{on} CO ($mM^{-1}s^{-1}$)	Reference
Mt-trHbN	4495	This work
Mt-trHbN VG8F	715	This work
Mt-trHbN VG8W	48	This work
Mt-trHbO	13 (79%) - 180 (21%) *	33
Mt-trHbO WG8F	3700 (75%) - 1200 (25%) *	12

*major and minor rate contributions to a biphasic fitting are indicated between brackets.

protein distal site cavity, ii) displacement of water molecules from the distal site cavity[15–17,35]. With this in mind, we performed classical MD simulations as they allow us to investigate both processes involved in ligand association. Ligand migration was studied using ILS calculations for the wild type, as well as both VG8F and VG8W mutant proteins. Displacement of retained water molecules in the distal site was considered by performing classical MD simulations and analyzing the solvation structure in each active site.

The wild type Mt-trHbN presents two tunnels available for ligand migration, the LT and the STG8 (Figure 4A). On the one hand, the LT connects three internal cavities: $(trHb : CO)_1$, $(trHb : CO)_2$ and $(trHb : CO)_3$. The STG8, on the other hand, has only the distal site cavity, $(trHb : CO)_1$, which is directly connected to the solvent. The VG8F mutant conserves both tunnels, although they are constrained compared to those in the wild type. In the VG8W case, however, the energy profiles suggest a completely blocked STG8 and a LT for which the accessibility to the iron heme is partially reduced.

In order to quantify the contribution of the single G8 mutation we computed free energy profiles for CO migration through both LT and STG8 tunnels (Figure 4B, 4C). The free energy was set to a value of 0 kcal/mol where CO ligand is fully solvated- at 13 Å and 24 Å from the Fe atom, for STG8 and LT respectively. Wild type Mt-trHbN presents small barriers (~2 kcal mol^{-1}) for CO migration from the solvent to the active site cavity $(trHb : CO)_1$ through both tunnels.

The active site water molecules occupancy was computed for all three systems by performing 200 ns of MD simulations with explicit water molecules. In each case a water molecule was able to access the active site and was stabilized by the iron and the distal site residues (Figure 5). Specifically, in both wild type and VG8F Mt-trHbN a water molecule was present for approximately 40% of the length of the simulation (Figure 5A, 5B). The VG8W mutant active site, on the other hand, is occupied by water molecules in 80% of the simulation time, probably due to the hydrogen bonding capacity of W (Figure 5C).

•NO decomposition in the presence of *M. tuberculosis* HbN

Mt-trHbN has previously been described as a dioxygenase, capable of O_2-dependent •NO consumption[36,37]. Consequently, •NO decomposition by purified Mt-trHbN and the VG8F, VG8W mutants was

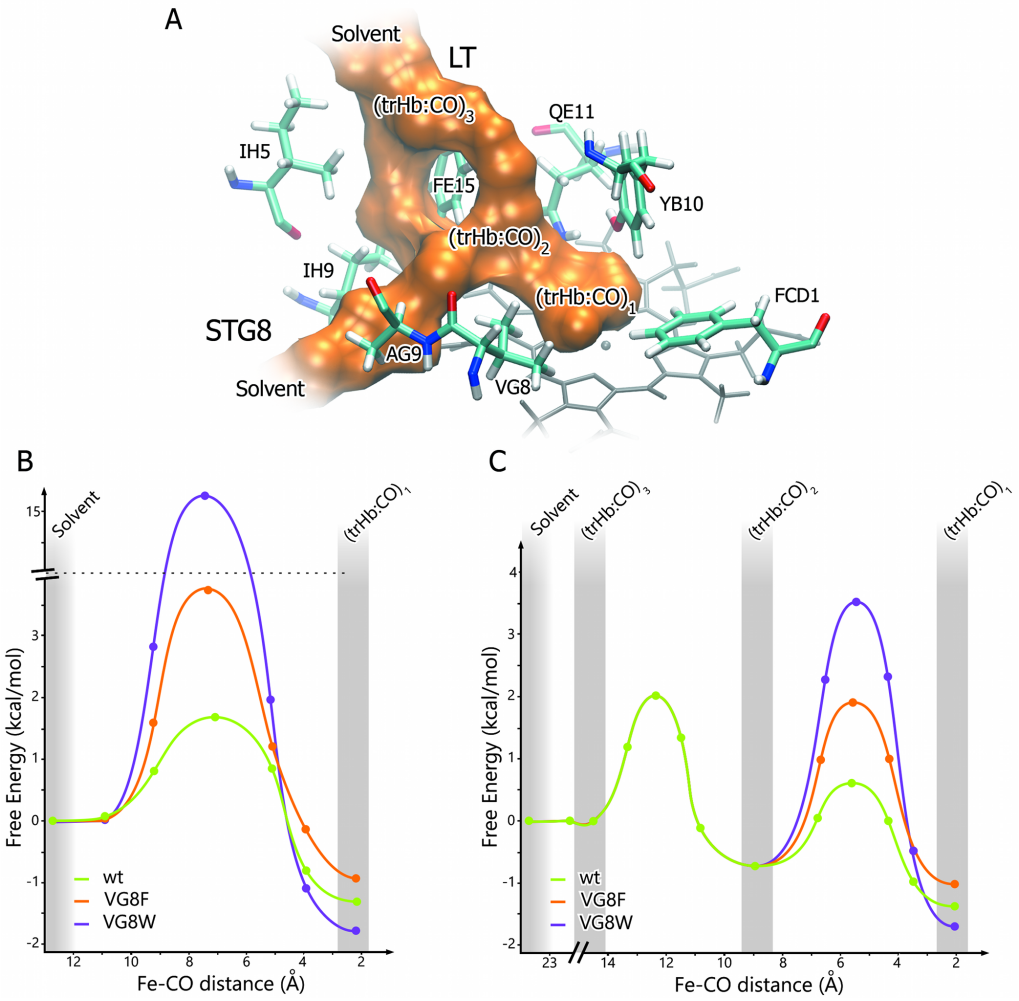

Figure 4. CO ligand migration along possible pathways in Mt-trHbN. (**A**) Schematic representations of the residues involved in the heme distal site and tunnels, the two tunnels and cavities estimated with ILS for the wild type form. (**B**) Free energy profiles over STG8 and (**C**) LT along the connection between solvent, $(trHb : CO)_2$ and $(trHb : CO)_1$ cavities for wild type (green), VG8F (orange) and VG8W (violet) mutant forms are shown. Circles represent calculated free energy values with the ILS method and lines correspond to a fitting estimation of these calculated values. The x coordinate represents the Fe-CO distance along the pathways.

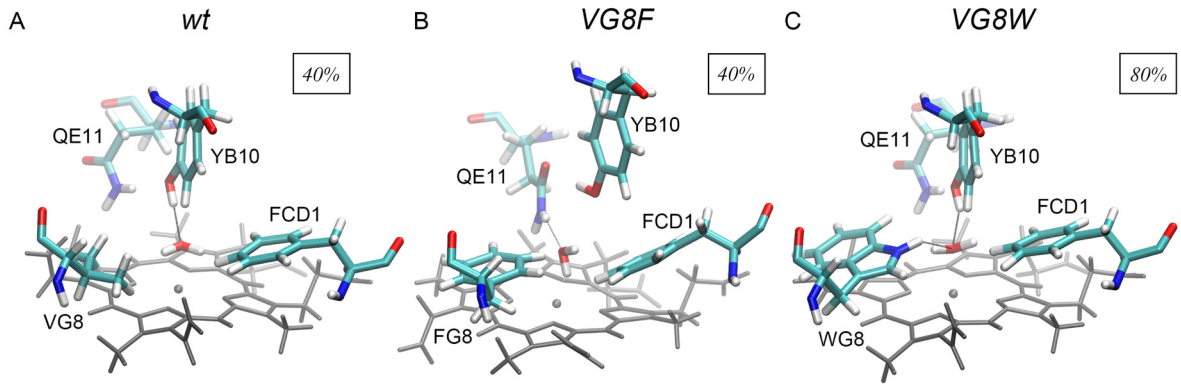

Figure 5. Schematic representations of the distal site of Mt-trHbN. (**A**) wild type, (**B**) VG8F and (**C**) VG8W forms showing, on the basis of MD simulations, the hydrogen-bond network (dotted lines) stabilizing a water molecule above the iron heme. The percentages depicted as insets in the figure correspond to active site water occupancy during MD simulation.

determined in a reaction mixture containing buffer, NADPH and *E. coli* FdR, to enable cyclic restoration of heme iron to the oxyferrous state. Figure 6A shows that in the absence of protein (red trace) decay of the •NO signal was monophasic until •NO was exhausted. The decay of NO in the presence of Mt-trHbN (black trace) was biphasic, with an almost linear initial rapid rate in decay, which was used to compare the various Mt-trHbN derivatives, followed by a slower rate in decay. This suggests that •NO is not being turned over in a cyclic manner, but is simply binding available heme. •NO consumption results show that the VG8F and VG8W mutans have a statistically significant reduced •NO binding capacity compared to HbN (Figure 6B).

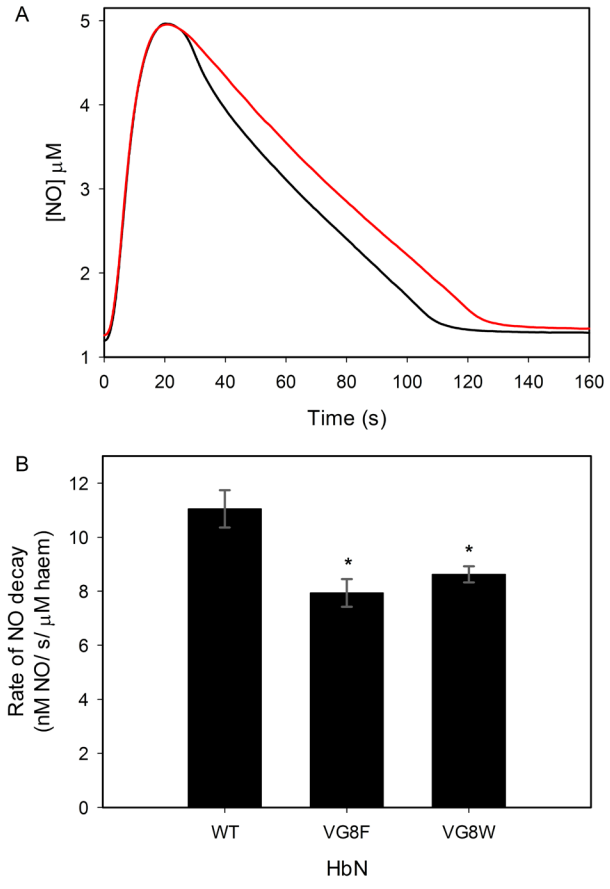

Figure 6. •NO decomposition by Mt-trHbN. (**A**) •NO decay was monitored amperometrically in the absence (red trace) and the presence (black trace) of Mt-trHbN added at the apex of the signal response to 2 µM ProliNONOate. Data are representative of 3 technical repeats. (**B**) Mean rates of •NO decay in the presence of wild type Mt-trHbN or site-directed mutants from 3 technical repeats ± S.E.M *$P < 0.05$, unpaired *t*-test.

Dataset 1. Experimental and theoretical calculations raw data

http://dx.doi.org/10.5256/f1000research.5921.d42091

Detailed legends describing the raw data can be found in the text file provided.

Discussion

CO association kinetic constant measurements as well as MD simulations of Mt-trHbN wild type and site-specific mutants were performed to analyze the role of tunnels and water molecules in the ligand association process. ILS calculations showed that the main tunnels of wild type Mt-trHbN, STG8 and LT, were partially blocked in the VG8F mutant and STG8 was nearly completely blocked in the VG8W mutant. The analysis of water molecules showed that VG8W increases the probablity of the presence of a water molecule in the distal site, which may interfere with the association process. Consistently, the association kinetic constants of CO for both Mt-trHbN mutants showed a decrease of slightly less than one order of magnitude when VG8 is replaced with F and two orders of magnitude when VG8 is replaced with W. Moreover, our data also showed that both mutants have less capacity of •NO binding than wild type Mt-trHbN.

Interestingly, the Mt-trHbN VG8W mutant presents a similar k_{on} CO to the wild type Mt-trHbO, showing that a single residue is responsible for the differential accessibility in these proteins. The results support the idea that STG8 and LT are the main channels for CO migration in the deoxygenated Mt-trHbN, as blocking these tunnels decreases the ability of CO to access the heme pocket. Although in both the mutated Mt-trHbN and wild type Mt-trHbO the STG8 is blocked by WG8, the LT remains open in Mt-trHbN, allowing CO access into the heme cavity, whereas the main tunnel for CO migration in Mt-trHbO is the E7, as was previously described[7]. This fact shows that although the k_{on} CO from mutant trHbN and wild type trHbO members are very similar, the ligand enters through different pathways, evidencing the complexity of mechanisms that regulate the ligand association process in these proteins.

Data availability

F1000Research: Dataset 1. Experimental and theoretical calculations raw data, 10.5256/f1000research.5921.d42091[39]

Author contributions

IB, LB, SC, RR, KLD, LAHB designed and performed the experiments. JPB, LB, MAM, DAE designed and analyzed the MD simulations. DAE, MAM, KSD and LB provided expertise in the field. KD, RLP, KLD, SS provided the experimental sample. JPB and LB wrote the manuscript. KSD, SS, LAHB, MTT and RP contributed to the experimental design and preparation of the manuscript. All

authors were involved in the revision of the draft manuscript and have agreed to the final content.

Competing interests

No competing interests were disclosed.

Grant information

This work was supported by Framework program 7 NOstress Grant, CONICET, University of Buenos Aires, and Agencia Nacional de Promoción Científica y Tecnológica, National Institutes of Health Grant R01AI095173 and Universidad de la República (CSIC, Uruguay) to R. R. Additional funding to SC and RR was provided by PEDECIBA (Progama de Desarrollo de Ciencias Básicas, Uruguay) and CeBEM (Centro de Biología Estructural del Mercosur). IB and JPB hold CONICET PhD fellowships. LB is a Pew Latin American Fellow. LB, DAE and MAM are members of CONICET.

I confirm that the funders had no role in study design, data collection and analysis, decision to publish, or preparation of the manuscript.

Acknowledgements

FJ Luque is acknowledged for useful discussions and suggestions. Mehrnoosh Arrar is acknowledged for close reading of the manuscript.

Supplementary material

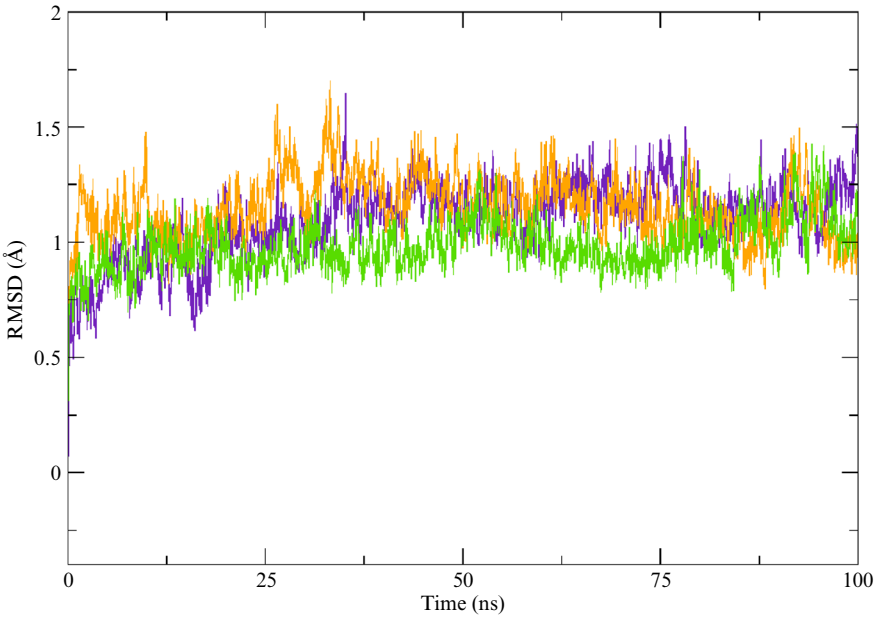

Figure S1. Root Mean Square Deviation during MD simulations for all the Mt-trHbN studied: wild type (green), VG8F (orange) and VG8W (violet).

References

1. Sudre P, ten Dam G, Kochi A: **Tuberculosis: a global overview of the situation today.** *Bull World Health Organ.* 1992; **70**(2): 149–159.
PubMed Abstract | Free Full Text

2. Milani M, Pesce A, Nardini M, *et al.*: **Structural bases for heme binding and diatomic ligand recognition in truncated hemoglobins.** *J Inorg Biochem.* 2005; **99**(1): 97–109.
PubMed Abstract | Publisher Full Text

3. Wittenberg JB, Bolognesi M, Wittenberg BA, *et al.*: **Truncated hemoglobins: a new family of hemoglobins widely distributed in bacteria, unicellular eukaryotes, and plants.** *J Biol Chem.* 2002; **277**(2): 871–874.
PubMed Abstract | Publisher Full Text

4. Ouellet H, Ouellet Y, Richard C, *et al.*: **Truncated hemoglobin HbN protects *Mycobacterium bovis* from nitric oxide.** *Proc Natl Acad Sci U S A.* 2002; **99**(9): 5902–5907.
PubMed Abstract | Publisher Full Text | Free Full Text

5. Crespo A, Martí MA, Kalko SG, *et al.*: **Theoretical study of the truncated hemoglobin, HbN: exploring the molecular basis of the NO detoxification mechanism.** *J Am Chem Soc.* 2005; **127**(12): 4433–4444.
PubMed Abstract | Publisher Full Text

6. Fabozzi G, Ascenzi P, Renzi SD, *et al.*: **Truncated hemoglobin GlbO from *Mycobacterium leprae* alleviates nitric oxide toxicity.** *Microb Pathog.* 2006; **40**(5): 211–220.
PubMed Abstract | Publisher Full Text

7. Boechi L, Mañez PA, Javier Luque FJ, *et al.*: **Unraveling the molecular basis for ligand binding in truncated hemoglobins: the trHbO *Bacillus subtilis* case.**

Proteins. 2010; **78**(4): 962–970.
PubMed Abstract | Publisher Full Text

8. Bidon-Chanal A, Martı MA, Crespo A, *et al.*: *Proteins.* 2007; **464**: 457–464.
9. Perutz MF, Mathews FS: **An X-ray study of azide methaemoglobin.** *J Mol Biol.* 1966; **21**(1): 199–202.
PubMed Abstract | Publisher Full Text
10. Boechi L, Arrar M, Marti MA, *et al.*: **Hydrophobic effect drives oxygen uptake in myoglobin via histidine E7.** *J Biol Chem.* 2013; **288**(9): 6754–62.
PubMed Abstract | Publisher Full Text | Free Full Text
11. Elber R: **Ligand diffusion in globins: simulations versus experiment.** *Curr Opin Struct Biol.* 2010; **20**(2): 162–167.
PubMed Abstract | Publisher Full Text | Free Full Text
12. Ouellet H, Milani M, LaBarre M, *et al.*: **The roles of Tyr(CD1) and Trp(G8) in *Mycobacterium tuberculosis* truncated hemoglobin O in ligand binding and on the heme distal site architecture.** *Biochemistry.* 2007; **46**(41): 11440–11450.
PubMed Abstract | Publisher Full Text
13. Boechi L, Martí MA, Milani M, *et al.*: **Structural determinants of ligand migration in *Mycobacterium tuberculosis* truncated hemoglobin O.** *Proteins.* 2008; **73**(2): 372–379.
PubMed Abstract | Publisher Full Text
14. Guallar V, Lu C, Borrelli K, *et al.*: **Ligand migration in the truncated hemoglobin-II from *Mycobacterium tuberculosis*: the role of G8 tryptophan.** *J Biol Chem.* 2009; **284**(5): 3106–3116.
PubMed Abstract | Publisher Full Text
15. Olson J, Phillips GN Jr: **Myoglobin discriminates between O_2, NO, and CO by electrostatic interactions with the bound ligand.** *J Biol Inorg Chem.* 1997; **2**: 544–552.
Publisher Full Text
16. Ouellet YH, Daigle R, Lagüe P, *et al.*: **Ligand binding to truncated hemoglobin N from *Mycobacterium tuberculosis* is strongly modulated by the interplay between the distal heme pocket residues and internal water.** *J Biol Chem.* 2008; **283**(40): 27270–27278.
PubMed Abstract | Publisher Full Text | Free Full Text
17. Bustamante JP, Abbruzzetti S, Marcelli A, *et al.*: **Ligand uptake modulation by internal water molecules and hydrophobic cavities in hemoglobins.** *J Phys Chem B.* 2014; **118**(5): 1234–45.
PubMed Abstract | Publisher Full Text
18. Rozen S, Skaletsky H: **Primer3 on the WWW for general users and for biologist programmers.** *Methods Mol Biol.* 2000; **132**: 365–86.
PubMed Abstract | Publisher Full Text
19. Wainwright LM, Wang Y, Park SF, *et al.*: **Purification and spectroscopic characterization of Ctb, a group III truncated hemoglobin implicated in oxygen metabolism in the food-borne pathogen *Campylobacter jejuni*.** *Biochemistry.* 2006; **45**(19): 6003–6011.
PubMed Abstract | Publisher Full Text | Free Full Text
20. Milani M, Pesce A, Ouellet Y, *et al.*: ***Mycobacterium tuberculosis* hemoglobin N displays a protein tunnel suited for O_2 diffusion to the heme.** *EMBO J.* 2001; **20**(15): 3902–3909.
PubMed Abstract | Publisher Full Text | Free Full Text
21. Pearlman DA, Case DA, Caldwell JW, *et al.*: *Comput Phys Commun.* 1995; **91**: 1–41.
22. Wang J, Cieplak P, Kollman, PA: **How well does a restrained electrostatic potential (RESP) model perform in calculating conformational energies of organic and biological molecules?** *J Comput Chem.* 2000; **21**(12): 1049–1074.
Publisher Full Text
23. Marti MA, Capece L, Bidon-Chanal A, *et al.*: **Nitric oxide reactivity with globins as investigated through computer simulation.** *Methods Enzymol.* 2008; **437**: 477–498.
PubMed Abstract | Publisher Full Text
24. Bikiel DE, Boechi L, Capece L, *et al.*: **Modeling heme proteins using atomistic simulations.** *Phys Chem Chem Phys.* 2006; **8**(48): 5611–5628.
PubMed Abstract | Publisher Full Text
25. Capece L, Lewis-Ballester A, Marti MA, *et al.*: **Molecular basis for the substrate stereoselectivity in tryptophan dioxygenase.** *Biochemistry.* 2011; **50**(50): 10910–10918.
PubMed Abstract | Publisher Full Text | Free Full Text
26. Forti F, Boechi L, Bikiel D, *et al.*: **Ligand migration in *Methanosarcina acetivorans* protoglobin: effects of ligand binding and dimeric assembly.** *J Phys Chem B.* 2011; **115**(46): 13771–13780.
PubMed Abstract | Publisher Full Text
27. Giordano D, Boechi L, Vergara A, *et al.*: **The hemoglobins of the sub-Antarctic fish Cottoperca gobio, a phyletically basal species--oxygen-binding equilibria, kinetics and molecular dynamics.** *FEBS J.* 2009; **276**(8): 2266–2277.
PubMed Abstract | Publisher Full Text
28. Nicoletti FP, Droghetti E, Howes BD, *et al.*: **H-bonding networks of the distal residues and water molecules in the active site of Thermobifida fusca hemoglobin.** *Biochim Biophys Acta* 2013; **1834**(9): 1901–1909.
PubMed Abstract | Publisher Full Text
29. Marti MA, Crespo A, Capece L, *et al.*: **Dioxygen affinity in heme proteins investigated by computer simulation.** *J Inorg Biochem.* 2006; **100**(4): 761–770.
PubMed Abstract | Publisher Full Text
30. Perissinotti LL, Marti MA, Doctorovich F, *et al.*: **A microscopic study of the deoxyhemoglobin-catalyzed generation of nitric oxide from nitrite anion.** *Biochemistry.* 2008; **47**(37): 9793–9802.
PubMed Abstract | Publisher Full Text
31. Cohen J, Olsen KW, Schulten K: **Finding gas migration pathways in proteins using implicit ligand sampling.** *Methods Enzymol.* 2008; **437**: 439–457.
PubMed Abstract | Publisher Full Text
32. Forti F, Boechi L, Estrin DA, *et al.*: **Comparing and combining implicit ligand sampling with multiple steered molecular dynamics to study ligand migration processes in heme proteins.** *J Comput Chem.* 2011; **32**(10): 2219–2231.
PubMed Abstract | Publisher Full Text
33. Ouellet H, Juszczak L, Dantsker D, *et al.*: **Reactions of *Mycobacterium tuberculosis* truncated hemoglobin O with ligands reveal a novel ligand-inclusive hydrogen bond network.** *Biochemistry.* 2003; **42**(19): 5764–5774.
PubMed Abstract | Publisher Full Text
34. Couture M, Yeh SR, Wittenberg BA, *et al.*: **A cooperative oxygen-binding hemoglobin from *Mycobacterium tuberculosis*.** *Proc Natl Acad Sci U S A.* 1999; **96**(20): 11223–11228.
PubMed Abstract | Publisher Full Text | Free Full Text
35. Ouellet Y, Milani M, Couture M, *et al.*: **Ligand interactions in the distal heme pocket of *Mycobacterium tuberculosis* truncated hemoglobin N: roles of TyrB10 and GlnE11 residues.** *Biochemistry.* 2006; **45**(29): 8770–8781.
PubMed Abstract | Publisher Full Text
36. Lama A, Pawaria S, Bidon-Chanal A, *et al.*: **Role of Pre-A motif in nitric oxide scavenging by truncated hemoglobin, HbN, of *Mycobacterium tuberculosis*.** *J Biol Chem.* 2009; **284**(21): 14457–14468.
PubMed Abstract | Publisher Full Text | Free Full Text
37. Pathania R, Navani N, Gardner A, *et al.*: **Nitric oxide scavenging and detoxification by the *Mycobacterium tuberculosis* haemoglobin, HbN in *Escherichia coli*.** *Mol Microbiol.* 2002; **45**(5): 1303–1314.
PubMed Abstract | Publisher Full Text
38. Martí MA, Bidon-Chanal A, Crespo A, *et al.*: **Mechanism of product release in NO detoxification from *Mycobacterium tuberculosis* truncated hemoglobin N.** *J Am Chem Soc.* 2008; **130**(5): 1688–1693.
PubMed Abstract | Publisher Full Text
39. Boron I, Bustamante JP, Davidge KS, *et al.*: **Experimental and theoretical calculations raw data.** *F1000Research.* 2015.
Data Source

Open Peer Review

Current Referee Status: ✓

Version 1

Referee Report 09 February 2015

doi:10.5256/f1000research.6326.r7468

✓ **Marco Nardini**
Department of Biosciences, University of Milan, Milan, Italy

This manuscript describes CO association kinetic constant measurements, •NO decomposition, and molecular dynamics simulations on the wild type truncated Hb from *Mycobacterium tuberculosis* (Mt-trHbN) and two mutants (VG8F and VG8W) which introduce modifications in the two-tunnel system of the protein. The data are then compared to those from Mt-trHbO, suggesting that ligand migration is regulated by the internal tunnel architecture as well as by water molecules stabilized in the active site.

Although the topic of the structure and the dynamic behavior of protein matrix tunnels in truncated Hb, and in particular in Mt-trHbN, has been “squeezed” a lot during the past years, the data reported in this paper add some new information and might be of interest in the field. The paper is well written (with regards to the requirements of the journal) and describes a technically sound piece of scientific research with data that supports the conclusions. Indexing is recommended, if the (few) minor comments below are addressed.

Minor remarks:

- Abstract: line 4
  The authors write that “Mt-trHbO” possesses tunnels that are partially blocked ..” In fact normally trHbOs are associated with internal discrete cavities and not with tunnels. The authors should rephrase the sentence.

- Abstract: line 11
  Mt-trHbN should not be in Italics.

- Abstract: line 12
  The sentence “mutations introduce modifications in both tunnel topologies” is quite cryptic and it is not clear what the author mean with “tunnel topologies”. The authors should rephrase the sentence to clarify it.

- Introduction: page 3, first column, line 8
  The authors might want to include a review on trHbs more recent than that indicated in reference (3). There are several of them published in the last few years.

- Introduction: page 3, first column, line 23
  The paragraph starting from line 23 is a bit misleading because the authors try to generalize the description of the protein matrix tunnels in trHbs by mixing what happens in trHbNs and trHbOs.

This is confusing since it might give the impression that three tunnels co-exist in trHbs, which is not true. In this respect, Figure 1 contributes a lot to make confusion, since it is not clear which trHb protein represents and it seems that it has three co-existing tunnels. It is probably better to keep separate trHbNs and trHbOs, both in the text description and in Figure 1. The authors should describe the tunnel features in trHbN (short and long tunnel) and trHbO (cavities, small E7 residues an possible E7 gating), and show two panels in Figure 1 with depicted the tunnel/cavity systems in Mt-trHbN (panel A) and Mt-trHbO (panel B), possibly using a similar protein orientation and highlighting the role of the G8 residue in the two cases.

- Introduction: page 3, second column, line 7
  The sentence regarding the “internal water molecules” is too generic as it is written now, since it is not clear if the authors refer to globins, to trHbs or to Mt-trHbs. The authors should rephrase the sentence to clarify this issue.

- Introduction: page 3, second column, line 10
  The authors should say that the experimental measurements and the MD simulations have been performed only on Mt-trHbN and mutants, and not, for instance, on Mt-trHbO.

- Materials and Methods: page 3, second column, line 40
  The purification paragraph seems to refers only to trHbN. What about its mutants? The authors should add a sentence to clarify this issue.

- Materials and Methods: page 4, first column, line 44
  The following sentence is not written fully correctly:
  “Amino acids protonation states were assumed based on environment of the residue in the crystal structure. All solvent-exposed His were protonated at the N- δ delta atom, as well as HisF8, because of its coordination to the heme iron”.

  One possibility is to rephrase it as follows:
  “The protonation state of the amino acids was assumed based on the environment of the residues in the crystal structure. All solvent-exposed His residues were protonated at the N-δ atom, as well as the proximal HisF8, because of its coordination to the heme iron”.

- page 5, second column, line 12
  It is not clear what the authors mean when they write that the STG8 “has only the distal site cavity, $(trHb : CO)_1$, …”, especially if this sentence is coupled with Figure 4A, where $(trHb : CO)_1$ seems to be connected to STG8 through $(trHb : CO)_2$.

- page 5, Title of Table 1
  It is probably better to change “..for wild type and mutants Mt-trHbs O and N” to “..for wild type and mutants of Mt-trHbN and Mt-trHbO”

- page 6, Figure 4 legend
  In the legend of Panel C there is no mention of the $(trHb : CO)_3$ site.

- References: page 9
  Reference (21) is missing the title

I have read this submission. I believe that I have an appropriate level of expertise to confirm that it is of an acceptable scientific standard.

Competing Interests: No competing interests were disclosed.